0026-895X/02/6205-1215–1227$7.00
MOLECULAR PHARMACOLOGY
Copyright © 2002 The American Society for Pharmacology and Experimental Therapeutics
Mol Pharmacol 62:1215–1227, 2002

Vol. 62, No. 5
1903/1021599
Printed in U.S.A.

DNA Binding and Topoisomerase I Poisoning Activities of Novel Disaccharide Indolocarbazoles

MICHAËL FACOMPRE, CAROLINA CARRASCO, PIERRE COLSON, CLAUDE HOUSSIER, JOHN D. CHISHOLM, DAVID L. VAN VRANKEN, and CHRISTIAN BAILLY

Institut National de la Santé et de la Recherche Médicale U-524 et Laboratoire de Pharmacologie Antitumorale du Centre Oscar Lambret, Lille, France (M.F., C.C., C.B.), Biospectroscopy Laboratory, Department of Chemistry, University of Liege, Belgium (P.C., C.H.); and Department of Chemistry, University of California, Irvine, California (J.D.C., D.L.V.V.)

Received June 5, 2002; accepted August 19, 2002

This article is available online at http://molpharm.aspetjournals.org

ABSTRACT

The antibiotics AT2433-A1 and AT2433-B1 are two indolocarbazole diglycosides related to the antitumor drug rebeccamycin known to stabilize topoisomerase I-DNA complexes. This structural analogy prompted us to explore the binding of four indolocarbazole diglycosides with DNA and their capacity to interfere with the DNA cleavage-reunion reaction catalyzed by topoisomerase I. The molecular basis of the drug interaction with double-stranded DNA and with purified chromatin, with particular emphasis on the role of the carbohydrate moiety, was investigated by means of complementary spectroscopic techniques, including surface plasmon resonance and electric linear dichroism. We compared the DNA binding properties, sequence recognition, and effects on topoisomerase I-mediated DNA relaxation and cleavage of AT2433-A1 bearing a 2,4-dideoxy-4-methylamino-L-xylose residue, its dechlorinated analog AT2433-B1, the diastereoisomer iso-AT2433-B1 with an inverted aminosugar residue, and compounds 5*H*-indolo[2,3-*a*]pyrrolo[3,4-*c*]carbazole-5,7(6*H*)-dione, 12-β-D-glucopyranosyl-12,13-dihydro-6-methyl (JDC-108) and 5*H*-indolo[2,3-*a*]pyrrolo[3,4-*c*]carbazole-5,7(6*H*)-dione, 12-(6-*O*-α-D-galacto-pyranosyl-β-D-glucopyranosyl)-12,13-dihydro-6-methyl (JDC-277) with an uncharged mono- and disaccharide, respectively. The two antibiotics AT2433-A1 and AT2433-B1 proved to be highly cytotoxic to leukemia cells and this may be a consequence of their tight intercalative binding to DNA, preferentially into GC-rich sequences as inferred from DNase I footprinting studies and surface plasmon resonance measurements. Like the diastereoisomer iso-AT2433-B1, they have no inhibitory effect on topoisomerase I, in contrast to the uncharged diglycoside JDC-277, which stimulates DNA cleavage by the enzyme mainly at TG sites, as observed with camptothecin. Cytotoxicity measurements with CEM and CEM/C2 human leukemia cell lines sensitive and resistant to camptothecin, respectively, also suggested that topoisomerase I contributes, at least partially, to the mechanism of action of the neutral diglycoside JDC-277 but not to that of the cationic AT2433 compounds. Together, the results indicate that sequence-selective DNA interaction and topoisomerase I inhibition is controlled to a large extent by the stereochemistry of the diglycoside moiety.

The microorganism *Actinomadura melliaura* produces the two antibiotics AT2433-A1 and AT2433-B1 that only differ by the presence of a chlorine atom on the indolocarbazole chromophore (Fig. 1). In both cases, the large heterocyclic ring system is substituted by a unique disaccharide consisting of a methoxyglucose and an aminosugar subunit, 2,4-dideoxy-4-methylamino-L-xylose. These two antibiotics were first isolated in 1989 (Golik et al., 1989; Matson et al., 1989) and their total synthesis was accomplished 10 years later (Chisholm et al., 1999; Chisholm and Van Vranken, 2000) but their mechanism of action remains largely unknown.

AT2433-A1 and -B1 are structurally analogous to the monosaccharide indolocarbazole antibiotic rebeccamycin (Fig. 1) produced by *Saccharothrix aerocolonigenes* (Nettleton et al., 1985; Bush et al., 1987). This natural product containing an uncharged methoxyglucose residue has profoundly inspired the development of antitumor agents targeting topoisomerase I, a ubiquitous enzyme essential to the control of DNA topology in cells. A large number of synthetic monosaccharide rebeccamycin analogs have been developed and a few of them, such as the drug NB-506 (also known as

This work was supported by research grants from the Ligue Nationale Contre le Cancer (Equipe labelisée LA LIGUE) (to C.B.) and the American Cancer Society (to D.L.V.V.) and a Marie Curie Fellowship of the European Community Program "Improving Human Research Potential and the Socio-economic Knowledge Base" under contract number HPMFCT-2000-00701 (to C.C.). Support by the "Actions Intégrées Franco-Belge, Program Tournesol" is acknowledged.

ABBREVIATIONS: SPR, surface plasmon resonance; DMSO, dimethyl sulfoxide; RU, response unit; CD, circular dichroism; P/D, phosphate/drug; ELD, electric linear dichroism; PI, propidium iodide; BrdU, bromodeoxyuridine; CPT, camptothecin; RRI, relative resistance index; JDC-108, 5*H*-indolo[2,3-*a*]pyrrolo[3,4-*c*]carbazole-5,7(6*H*)-dione, 12-β-D-glucopyranosyl-12,13-dihydro-6-methyl; JDC-277, 5*H*-indolo[2,3-*a*]pyrrolo[3,4-*c*]carbazole-5,7(6*H*)-dione, 12-(6-*O*-α-D-galactopyranosyl-β-D-glucopyranosyl)-12,13-dihydro-6-methyl; NB-506, 6-*N*-formylamino-12,13-dihydro-1,11-dihydroxy-13-(β-D-glucopyranosyl)-5*H*-indolo[2,3-*a*]pyrrolo-[3,4-*c*]carbazole-5,7-(6*H*)-dione.

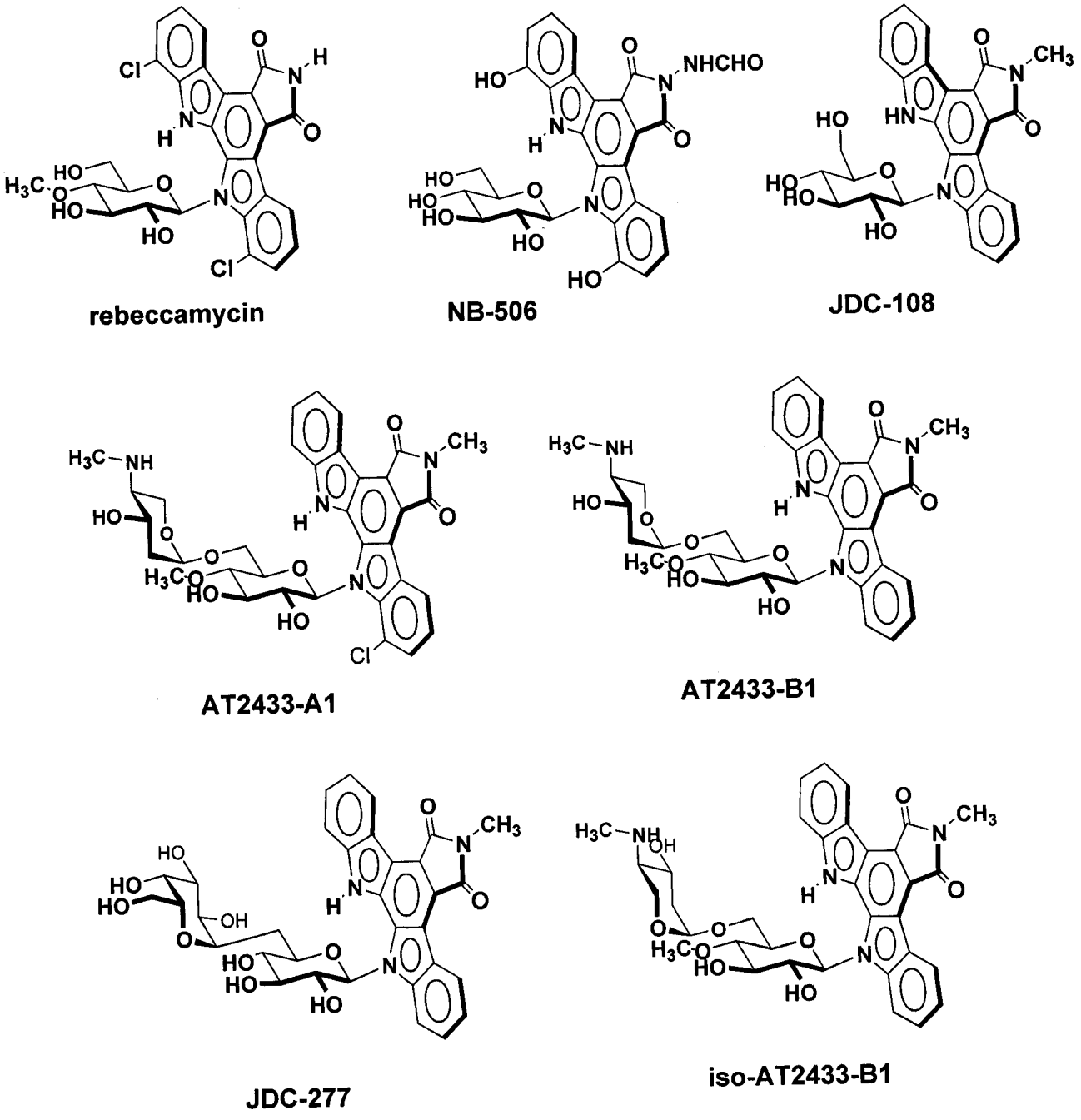

Fig. 1. Structures of the mono- and bis-glycosylated indolocarbazole derivatives used in this study.

J-107185 or L-753,000; Fig. 1), have revealed promising anticancer activities in vivo (Arakawa et al., 1995; Kanzawa et al., 1995; Yoshinari et al., 1995). Topoisomerase I is a primary target for NB-506 and related monosaccharide compounds (Urasaki et al., 2001; Woo et al., 2002).

The structural analogy between AT2433-A1 and rebeccamycin prompted us to postulate that the disaccharide antibiotics can also bind to DNA and interfere with the DNA cleavage activity of topoisomerase I. To test this hypothesis and investigate the structure-activity relationships in the indolocarbazole disaccharide series, we selected four compounds, AT2433-A1, AT2433-B1, iso-AT2433-B1, and the compound JDC-277, with an uncharged D-melibiose sugar unit (Fig. 1). Iso-AT2433-B1 is a diastereoisomer of the natural aminodisaccharide and corresponds to the incorrect structure originally proposed for AT2433-B1 (Chisholm et al., 1999). The four diglycosides contain the same *N*-methyl indolo[2,3-*a*]carbazole chromophore and for this reason, we choose the D-glucose derivative JDC-108 as a control monoglycoside (Fig. 1). A range of biophysical and biochemical techniques was used to compare the effects of these compounds on DNA and topoisomerase I at the molecular and cellular levels.

Materials and Methods

Drugs. The syntheses of the antibiotics AT2433-A1/B1 and the analogs used in this study have been described previously (Chisholm

et al., 1999; Chisholm and Van Vranken, 2000). Camptothecin was purchased from Sigma-Aldrich (St. Louis, MO) and a sample of NB-506 (J-107185) was kindly provided by Dr. Tomoko Yoshinari (Banyu Pharmaceutical Co., Ltd., Tsukuba, Japan). Except for the surface plasmon resonance (SPR) experiments, the drugs were dissolved in DMSO at 5 mM. The stock DMSO solutions of drugs were kept at −20°C and freshly diluted with water to the desired concentration immediately before use.

Absorption Spectra and Melting Temperature Studies. Melting curves were measured using an Uvikon 943 spectrophotometer (Kontron, Zurich, Switzerland) coupled to a Neslab RTE111 cryostat. For each series of measurements, 12 samples were placed in a thermostatically controlled cell-holder, and the quartz cuvettes (10-mm pathlength) were heated by circulating water. Measurements were performed in BPE buffer, pH 7.1 (6 mM Na_2HPO_4, 2 mM NaH_2PO_4, and 1 mM EDTA). The temperature inside the cuvette was measured with a platinum probe; it was increased over the range 20–100°C with a heating rate of 1°C/min. The "melting" temperature, *T*m, was taken as the mid-point of the hyperchromic transition. The Uvikon 943 spectrophotometer was also used to record the absorption spectra.

Surface Plasmon Resonance. The 5′ biotin-labeled DNA hairpins d(CATATATATCCCCATATATATG) and d(CGCGCGCGTTTTCGCGCGCG) (hairpin loop underlined, polyacrylamide gel electrophoresis-purified; Eurogentec, Seraing, Belgium) were used for the SPR studies. Samples of hairpin DNA oligomers in HBS-EP buffer (10 mM HEPES, pH 7.4, 150 mM NaCl, 3 mM EDTA, and 0.0005% Surfactant P20) at 25 nM concentration were applied to flow cells in streptavidin-derivatized sensor chips (BiaCore SA-chips; BiaCore, Uppsala, Sweden) by direct flow at 2 μl/min in a four-channel 3000 optical biosensor system (BiaCore). The sensor chips were conditioned with three consecutive 1-min injections of 1 M NaCl in 50 mM NaOH followed by extensive washing with buffer. Nearly the same amount of all oligomers was immobilized on the surface by noncovalent capture, leaving one of the flow cells blank as a control. Manual injection was used with a flow rate of 2 μl/min to achieve long contact times with the surface and to control the amount of the DNA bound to the surface. All procedures for binding studies were automated as methods using repetitive cycles of sample injection and regeneration. Steady-state binding analysis was performed with multiple injections of different compound concentrations over the immobilized DNA surfaces for a 10-min period at a flow rate of 20 μl/min and 25°C. Solutions of drug with known concentrations were prepared in filtered and degassed buffer by serial dilutions from stock solution and were injected from 7-mm plastic vials with pierceable plastic crimp caps (BiaCore).

The instrument response [as measured in response units (RU)] in the steady-state region is proportional to the amount of bound drug and was determined by linear averaging over an 80-s time span. The predicted maximum response per bound compound in the steady-state region (RU_{max}) is determined from the DNA molecular weight, the amount of DNA on the flow cell, the compound molecular weight, and the refractive index gradient ratio of the compound and DNA, as described previously (Davis and Wilson, 2000). The number of binding sites was determined from Scatchard plots derived from plots of RU/concentration versus RU plot using a linear regression analysis (data not shown). The RU_{max} value is required to convert the observed response (RU) to the standard binding parameter, r (moles of drug bound/moles of DNA hairpin) by using the equation $r = RU/RU_{max}$.

Average fitting of the sensorgrams at the steady-state level was performed with the BIAevaluation 3.0 program (BIAcore, Uppsala, Sweden). To obtain the affinity constants, the results from the steady-state region were fitted with a multiple equivalent-site model using Kaleidagraph (Synergy Software, Reading, PA) for nonlinear least-squares optimization of the binding parameters with the following equation: $r = n \times K \times C_{free}/(1 + K \times C_{free})$, where K, the macroscopic binding constant, is one variable to fit; r represents the moles of bound compound per mole of DNA hairpin duplex; C_{free} is the concentration of the compound in equilibrium with the complex and is fixed by the concentration in the flow solution; and n is the number of compound binding sites on the DNA duplex, and is the second variable to fit. The r values are calculated by the ratio RU/RU_{max} where RU is the steady-state response at each concentration and RU_{max} is the predicted RU for binding of a single compound to the DNA on a flow cell.

Circular Dichroism. Circular dichroic (CD) spectra were recorded on a J-810 dichrograph (Jasco, Tokyo, Japan). Solutions of drugs, nucleic acids, and their complexes (1 ml in 1 mM sodium cacodylate buffer, pH 7.0) were scanned in 1-cm quartz cuvettes. Measurements were made by progressive dilution of drug-DNA complex at a high phosphate/drug (P/D) ratio with a pure ligand solution to yield the desired drug/DNA ratio. Three scans were accumulated and automatically averaged.

Preparation of Chromatin Fibers and Electric Linear Dichroism. The chromatin was extracted from chicken erythrocytes and purified according to procedures described in Hagmar et al. (1989). The alternating double-stranded polymers $poly(dAT)_2$ and $poly(dGC)_2$ (Pharmacia AB, Uppsala, Sweden) were used without further purification. Calf thymus DNA was deproteinized with sodium dodecyl sulfate (protein content <0.2%) and all nucleic acids were dialyzed against 1 mM sodium cacodylate buffered solution, pH 7.0. Details of the procedures used for electric linear dichroism (ELD) experiments were reported previously (Bailly et al., 1990; Colson et al., 1996). In the ionic strength conditions used for ELD measurements, chromatin (10–80 nucleosomes long) is mostly present as the 10-nm fiber. The optical setup incorporating a high sensitivity T-jump instrument equipped with a Glan polarizer was used under the following conditions: bandwidth, 3 nm, sensitivity limit, 0.001 in ΔA/A; and response time, 3 μs. All experiments were conducted at 20°C with a 10-mm pathlength Kerr cell having 1.5-mm electrode separation (Houssier, 1981).

Purification and Radiolabeling of DNA Restriction Fragments. The 117- and 265-base pair DNA fragment were prepared by 3′-^{32}P-end labeling of the *Eco*RI-*Pvu*II double digest of the plasmid pBS (Stratagene, La Jolla, CA) using α-[^{32}P]dATP (3000 Ci/mmol) and avian myeloblastosis virus reverse transcriptase. The same procedure was applied for the 174-mer *Eco*RI-*Pvu*II fragment from plasmid pKS (Stratagene). In each case, the digestion products were separated on a 6% polyacrylamide gel under native conditions in Tris-borate/EDTA-buffered solution (89 mM Tris-borate, pH 8.3, and 1 mM EDTA). After autoradiography, the band of DNA was excised, crushed, and soaked in water overnight at 37°C. This suspension was filtered through a 0.22-μm filter (Millipore Corporation, Bedford, MA) and the DNA was precipitated with ethanol. After washing with 70% ethanol and vacuum drying of the precipitate, the labeled DNA was resuspended in 10 mM Tris adjusted to pH 7.0 containing 10 mM NaCl.

DNase I Footprinting, Electrophoresis, and Quantitation by Storage Phosphorimaging. Experiments were performed essentially as described previously (Bailly and Waring, 1995). Briefly, reactions were conducted in a total volume of 10 μl. Samples (3 μl) of the labeled DNA fragments were incubated with 5 μl of the buffered solution containing the ligand at appropriate concentration. After 30-min incubation at 37°C to ensure equilibration of the binding reaction, the digestion was initiated by the addition of 2 μl of a DNase I solution whose concentration was adjusted to yield a final enzyme concentration of about 0.01 unit/ml in the reaction mixture. After 3 min, the reaction was stopped by freeze drying. Samples were lyophilized and resuspended in 5 μl of an 80% formamide solution containing tracking dyes. The DNA samples were then heated at 90°C for 4 min and chilled in ice for 4 min before electrophoresis.

DNA cleavage products were resolved by polyacrylamide gel electrophoresis under denaturating conditions (0.3 mm in thickness, 8% acrylamide containing 8 M urea). After electrophoresis (about 2.5 h at 60 W, 1600 V in Tris borate-EDTA-buffered solution), gels were

soaked in 10% acetic acid for 10 min, transferred to 3MM paper (Whatman, Maidstone, England), and dried under vacuum at 80°C. A 425E PhosphorImager (Amersham Biosciences, Piscataway, NJ) was used to collect data from the storage screens exposed to dried gels overnight at room temperature. Baseline-corrected scans were analyzed by integrating all the densities between two selected boundaries using ImageQuant version 3.3 software (Amersham Biosciences). Each resolved band was assigned to a particular bond within the DNA fragments by comparison of its position relative to sequencing standards generated by treatment of the DNA with dimethyl sulfate followed by piperidine-induced cleavage at the modified guanine bases in DNA (G-track).

Sequencing of Topoisomerase I-Mediated DNA Cleavage Sites. Each reaction mixture contained 2 μl of 3′ end ^{32}P-labeled DNA (~1 μM), 5 μl of water, 2 μl of 10× topoisomerase I buffer, and 10 μl of drug solution at the desired concentration (1–100 μM). After 10-min incubation to ensure equilibration, the reaction was initiated by addition of 2 μl (20 units) of calf thymus topoisomerase I (Invitrogen, Carlsbad, CA). Samples were incubated for 45 min at 37°C before adding SDS to 0.25% and proteinase K to 250 μg/ml to dissociate the drug-DNA-topoisomerase I-cleavable complexes. The DNA was precipitated with ethanol and then resuspended in 5 μl of formamide-Tris borate-EDTA loading buffer, denatured at 90°C for 4 min, and then chilled in ice for 4 min before loading on to the sequencing gel. DNA cleavage products were resolved by polyacrylamide gel electrophoresis under denaturing conditions, as described above for the footprinting experiments.

DNA Relaxation Experiments. Supercoiled pKMp27 DNA (0.5 μg) was incubated with 4 units of human topoisomerase I or II (TopoGEN, Columbus, OH) at 37°C for 1 h in relaxation buffer (50 mM Tris pH 7.8, 50 mM KCl, 10 mM $MgCl_2$, 1 mM dithiothreitol, and 1 mM EDTA) in the presence of varying concentrations of the drug under study. Reactions were terminated by adding SDS to 0.25% and proteinase K to 250 μg/ml. DNA samples were then added to the electrophoresis dye mixture (3 μl) and electrophoresed in a 1% agarose gel at room temperature for 2 h at 120 V. Gels were stained with ethidium bromide (1 μg/ml), washed, and photographed under UV light. Similar experiments were performed using ethidium-containing agarose gels.

Cell Cultures and Survival Assay. Human CEM and CEM/C2 leukemia cells were obtained from the American Type Culture Collection (Manassas, VA). Cells were grown at 37°C in a humidified atmosphere containing 5% CO_2 in RPMI 1640 medium, supplemented with 10% fetal bovine serum, L-glutamine (2 mM), 1.5 g/l sodium bicarbonate, 4.5 g/l glucose, 10 mM HEPES, 1 mM sodium pyruvate, 100 IU/ml penicillin, and 100 μg/ml streptomycin. The cytotoxicity of the test compounds was assessed using a cell proliferation assay developed by Promega (Madison, WI) (CellTiter 96 AQ_{ueous} one solution cell proliferation assay). Briefly, 3×10^4 exponentially growing cells were seeded in 96-well microculture plates with various drug concentrations in a volume of 100 μl. After 72-h incubation at 37°C, 20 μl of the tetrazolium dye was added to each well and the samples were incubated for a further 2 h at 37°C. Plates were analyzed on a Multiskan MS (type 352) reader (Labsystem, Helsinki, Finland) at 492 nm.

Cell Cycle Analysis. For flow cytometric analysis of DNA content, 10^6 cells in exponential growth were treated with graded concentrations of the test drug for 24 h and then washed three times with citrate buffer. The cell pellet was incubated with 250 μl of trypsin-containing citrate buffer for 10 min at room temperature and then with 200 μl of citrate buffer containing a trypsin inhibitor and RNase (10 min) before adding 200 μl of propidium iodide (PI) at 125 μg/ml. Samples were analyzed on a FACScan flow cytometer (BD Biosciences, San Jose, CA) using the LYSYS II software, which is also used to determine the percentage of cells in the different phases of the cell cycle. PI was excited at 488 nm, and fluorescence was analyzed at 620 nm on channel Fl-3.

Bromodeoxyuridine Incorporation. Cells were cultured in complete RPMI 1640 medium with the test drug at different concentrations for 24 h before harvesting and then pulse-labeled with 10 μM BrdU for 60 min in complete medium. After two washes in phosphate-buffered saline, pH 7.3, with 0.1% sodium azide, cells were fixed in ethanol 70% and incubated 1 h at 4°C. After another wash in phosphate-buffered saline, cells were denatured in 2 N HCl for 15 min at 37°C (or 30 min at room temperature) under gentle stirring. pH was adjusted by a short incubation (5 min) in 3 ml of 0.1 M $Na_2B_4O_7$, pH 8.5, before centrifugation (5 min, 500g, 4°C). The cell pellet was then washed with 5 ml of buffer containing phosphate-buffered saline, 0.05% Tween, and 0.1% bovine serum albumin (fraction V), resuspended in 50 μl of this buffer, and then incubated with the fluorescein isothiocyanate-conjugated anti-BrdU monoclonal antibody (BD Biosciences) for 30 min at room temperature in the dark. For the negative controls, the pellet was incubated without antibody. All cell pellets were washed with 1 ml of buffer containing phosphate-buffered saline, 0.05% Tween, and 0.1% bovine serum albumin. Cells were collected by centrifugation and counterstained with 10 μg/ml of propidium iodide and treated with RNase (1 μg/ml). Samples were analyzed on a FACScan flow cytometer (BD Biosciences) using the LYSYS II software.

Results

DNA Binding Affinities. Different spectroscopic methods were used to compare the affinity of the drugs for DNA. Absorption measurements provided the first indication that the test compounds exhibit distinct binding affinities. Figure 2A shows the absorption spectra of AT2433-B1 and JDC-277 in the absence and presence of calf thymus DNA. The extent of hypochromism at the composite band with two maxima at 287 and 317 nm is much higher with AT2433-B1 compared with JDC-277 and the bathochromism is slightly more pronounced (8 versus 4 nm). Melting temperature measurements also suggested that the DNA affinity of AT2433-B1 is significantly higher than that of JDC-277. The histograms in Fig. 3 compare the ΔTm values ($\Delta T\text{m} = T\text{m}^{\text{complex}} - T\text{m}^{\text{DNA}}$) values measured with each drug interacting with calf thymus

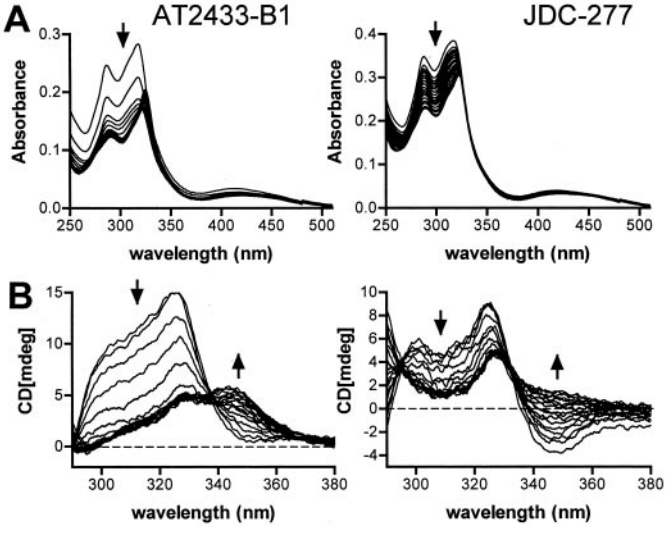

Fig. 2. Absorption (A) and circular dichroism spectra (B) of AT2433-B1 and JDC-277 in the presence of increasing concentrations of calf thymus DNA. DNA titrations of the drugs were performed in 1 mM sodium cacodylate buffer at pH 7.0. To 3 ml of drug solution at 20 μM was added aliquots of a concentrated calf thymus DNA solution. The phosphate-DNA/drug ratio increased from 0 to 20 in the direction indicated by the arrows.

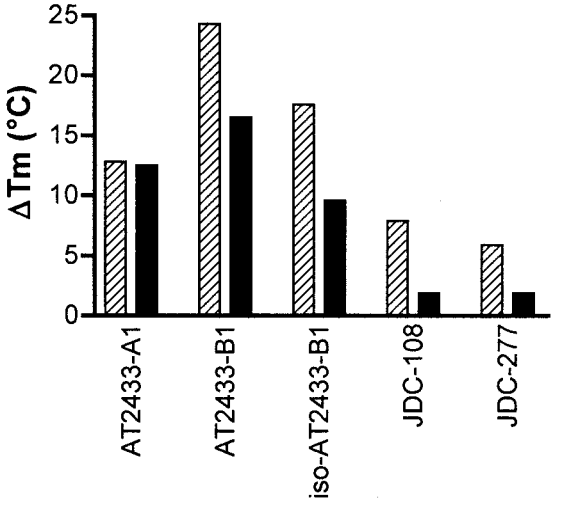

Fig. 3. Variation of the ΔTm ($Tm^{\text{drug-DNA complex}} - Tm^{\text{DNA alone}}$, in °C) of the complexes between the test compounds and (■) calf thymus DNA or (▨) poly(dAT)$_2$. Melting temperature measurements were performed in BPE buffer at pH 7.0 with a drug/DNA ratio of 0.5.

DNA or the polynucleotide poly(dAT)$_2$ at a drug/DNA-phosphate ratio of 0.5. AT2433-B1 stabilizes duplex DNA against heat denaturation more strongly than its chlorinated analog AT2433-A1 and the neutral mono- and bis-glycosyl compounds are much less efficient than the analogs containing an amino-diglycoside. This is the first indication that the chemical structure of the sugar unit is essential for DNA binding.

A quantitative analysis of the drug-DNA interaction was performed by SPR using a streptavidin-coated sensor chip. Two 5′ biotin-labeled hairpin oligomers containing an [AT]$_4$ or a [CG]$_4$ tract were immobilized on the sensor surface through streptavidin-biotin coupling and a blank flow cell was used as a control. To provide a signal directly proportional to the amount of bound compound, the reference response of this blank cell was subtracted from the response in the DNA channel. This highly sensitive method essentially requires water-soluble compounds to avoid problems due to the change of the refraction index with a solvent such as DMSO. We were able to prepare dilute aqueous solutions of the bisglycosyl compounds but not for JDC-108 bearing only

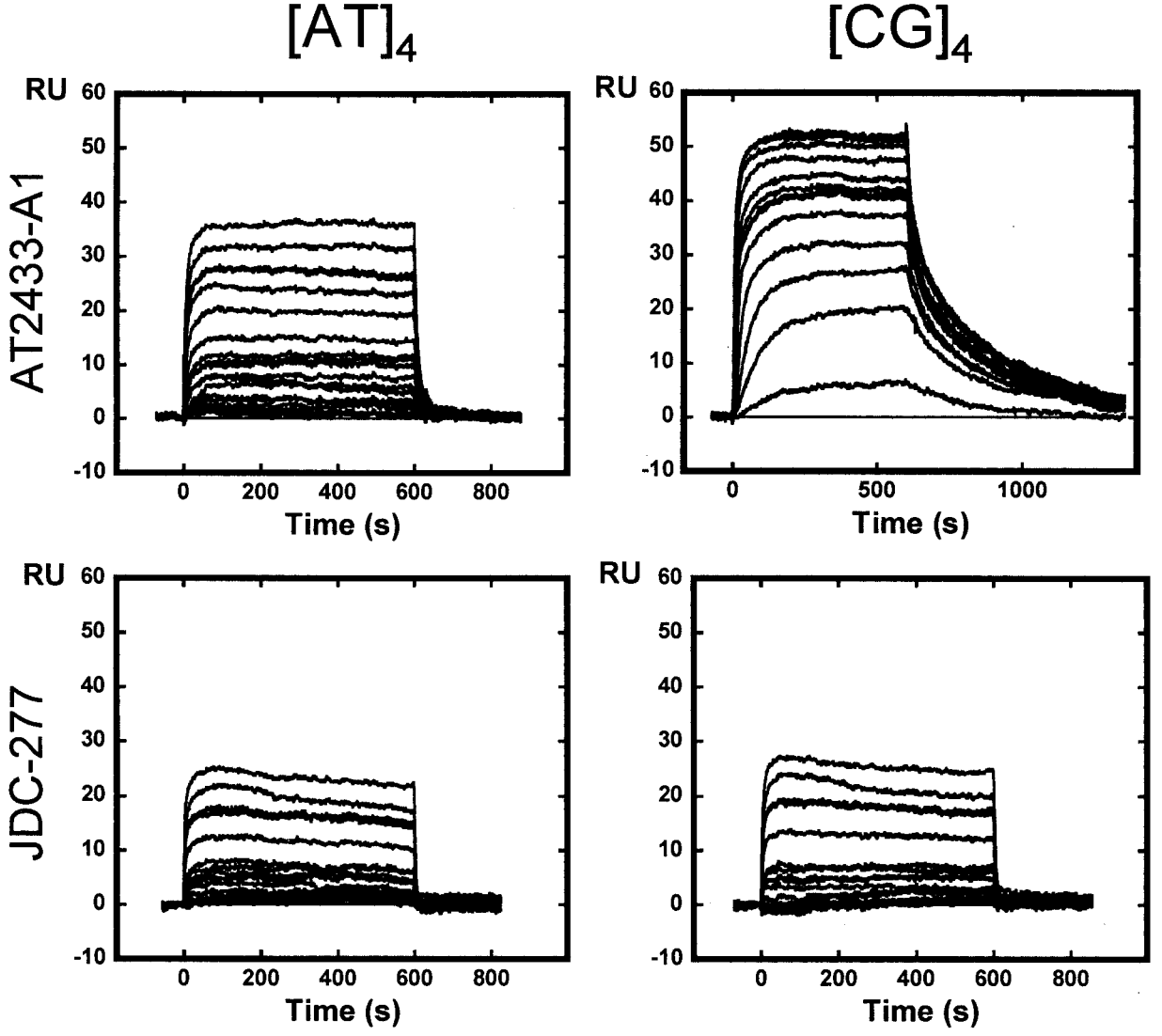

Fig. 4. SPR sensorgrams for binding of AT2433-A1 and JDC-277 to the [AT]$_4$ and [CG]$_4$ DNA hairpin oligomers in HBS-EP buffer. In each case, the concentration of the unbound ligand in the flow solution varies from 0 to 5 μM (top curve).

one sugar unit and therefore this compound could not be used for the SPR analysis. Representative SPR sensorgrams at different concentrations of AT2433-A1 and JDC-277 binding to the AT and GC duplexes are shown in Fig. 4. Similar sensorgrams were obtained with the two other compounds [see Carrasco et al. (2002) for a detailed analysis with AT2433-B1 and its diastereoisomer].

The amount of JDC-277 molecules bound to the two duplexes is weak compared with what can be achieved with AT2433-A1 (compare the RU values for a given concentration in Fig. 4). In addition, JDC-277-oligonucleotide complexes dissociate rapidly with the buffer injection, whereas the complexes between AT2433-A1 and the $[CG]_4$ duplex dissociate considerably more slowly. Interestingly, AT2433-A1 shows a clear preference for the GC duplex (tight binding and slow kinetics) compared with the AT duplex (weaker binding and fast kinetics). For each drug, the sensorgram results were fitted in the steady-state region as described under *Materials and Methods* and the measured binding constants (K_{eq}) are collected in Table 1. The equilibrium binding constant for AT2433-A1 binding to the $[CG]_4$ duplex DNA is more than 10 times higher than those measured with JDC-277 and iso-AT2433-B1, indicating most clearly that the DNA interaction is driven to a large extent by the nature of the sugar residue. The data obtained with AT2433-B1 and its diastereoisomer iso-AT2433-B1 are fully consistent with those recently reported in a detailed SPR study where we concluded that the amino sugar residue is an essential element that governs the DNA recognition process (Carrasco et al., 2002). The comparison of AT2433-B1 and -A1 indicates that the presence of a single chlorine atom on the indolocarbazole chromophore is sufficient to weaken the drug-DNA binding process. AT2433-A1 binds significantly less tightly to DNA that AT2433-B1 but still prefers the GC to the AT duplexes. In other words, the chlorine atom reduces DNA affinity but does not hinder sequence selectivity. This is consistent with the idea that binding strength is provided by the planar chromophore (adding a Cl group will restrict DNA intercalation), whereas sequence recognition is conferred by the carbohydrate moiety. These SPR data are in agreement with the *T*m data reported above and the subsequent footprinting results.

DNA Binding Mode. Two spectroscopic methods using polarized light, CD and ELD, were deployed to investigate the orientation of the indolocarbazole chromophore with respect to the DNA helix. The CD spectra for AT2433-B1 and JDC-277 interacting with DNA (Fig. 2B) confirm the weaker binding of the neutral disaccharide compared with the cationic parent compound. For both compounds, the decrease of the CD band at 300 to 330 nm is concomitant to an increase of the CD amplitude at 340 to 360 nm, with a relatively well resolved isodichroic crossover. This type of CD behavior may be assigned to excitonic coupling between adjacent intercalated molecules. The ELD measurements also strongly suggest intercalation. The dependence of the reduced dichroism

TABLE 1
Equilibrium binding constants determined by SPR
Experiments were performed in HBS-EP buffer at 25°C. The DNA sequences show one strand of the duplex stem of the hairpin used in the BIAcore SPR experiments. In each case, the number of compound binding sites on the DNA duplex is indicated (*n*).

DNA	K_{eq}			
	AT2433-A1	AT2433-B1	iso-AT2433-B1	JDC-277
	M^{-1}			
$[AT]_4$	$6.7\ 10^5$ (2)	$1.3\ 10^6$ (4–5)	$1.4\ 10^5$ (6–8)	$1.0\ 10^5$ (4)
$[CG]_4$	$6.6\ 10^6$ (3)	$8.9\ 10^6$ (3)	$5.0\ 10^5$ (4–6)	$5.0\ 10^5$ (4)

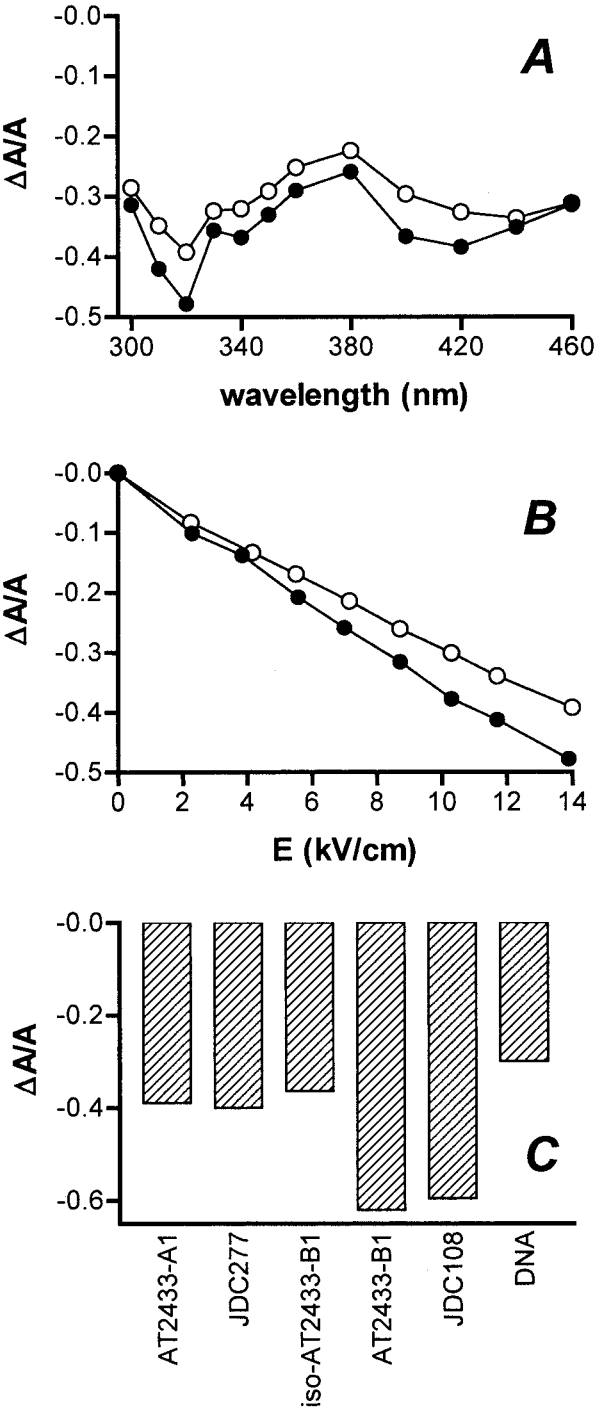

Fig. 5. ELD data for the binding to DNA. Dependence of the reduced dichroism ΔA/A on the wavelength (A) and electric field strength (B) for AT2433-B1 (●) and JDC-277 (○). Conditions: 13.6 kV/cm, P/D = 20 (200 μM DNA, 10 μM drug) (A); and 320 nm, P/D = 20 for the DNA-drug complexes and 260 nm for the DNA alone (B). C, variation of the reduced dichroism (ΔA/A) of the complexes between calf thymus DNA and the test compounds. ΔA/A was measured in the absorption band of the ligand-DNA complex (320 nm) or at 260 nm for DNA alone, at 13.5 kV/cm and at a DNA/drug ratio of 25. All measurements were performed in 1 mM sodium cacodylate buffer, pH 7.0.

(ΔA/A) on the wavelength and the electric field is shown in Fig. 5, A and B, for AT2433-B1 and JDC-277. For each drug-DNA complex (at a DNA/drug ratio of 25), ΔA/A was measured at 320 nm and compared with that obtained with calf thymus DNA alone at 260 nm (Fig. 5C). In all cases, negative ΔA/A values were measured, as expected for intercalating agents. With compounds AT2433-A1, JDC-277, and iso-AT2433-B1, the reduced dichroism was close to that of DNA alone, whereas more negative ΔA/A values were obtained with AT2433-B1 and JDC-108. The difference most likely reflects the stronger binding capacity of these two compounds, as indicated by the *T*m, SPR, and CD data. Although the amplitude of the ELD signals differs from one compound to another, the reduced dichroism is always negative in sign in the 300- to 350-nm region where the indolocarbazole chromophore absorbs the light and this is characteristic of an intercalative binding mode to DNA. It is possible that the indolocarbazole unit of the antibiotic is more tilted with respect to the base pair plane than that of JDC-277, or the two drugs exert different stiffening and unwinding effects on the DNA helix, but both compounds can be considered as DNA intercalators.

To determine the influence of proteins bound to DNA on the binding characteristics of the drugs, we studied their interaction with chromatin purified from chicken erythrocyte (Fig. 6). As with naked DNA, the ELD signal depends on the local orientation of the light-absorbing chromophores relative to the orientation axis of the macromolecule. Upon binding to chromatin fibers, the ligands all display negative ΔA/A values at 320 nm and assuming, by virtue of electrodynamic arguments (Hagmar et al., 1989), that the chromatin fibers are parallel to the electric field, the negative sign of the dichroism in the 320-nm band of the drugs, and of the DNA at 260 nm suggests an intercalation of the indolocarbazole moiety. The comparison of the chromatin binding capacities of AT2433-B1 and JDC-277 (Fig. 6) gave results comparable with those obtained with calf thymus DNA. The ELD spectra and the dependence of the reduced dichroism upon the chromatin/drug ratio shows unambiguously that the antibiotic exhibits a much higher capacity to intercalate into chromatin fibers than its uncharged derivative. The field strength dependence of the reduced dichroism of the chromatin-AT2433-B1 complexes is also unequivocal in that the dichroism amplitude of these complexes is higher (more negative) than that of the JDC-277-chromatin complexes. Together, the results suggest that the five drugs adopt a similar configuration upon binding to naked DNA and chromatin. The mode of interaction of JDC-277 and AT2433-B1 with chromatin remains qualitatively similar to that observed with naked DNA. Therefore, considering that the presence of histones does not alter the intercalation DNA-binding process, we can envisage that the presence of a DNA binding protein such as topoisomerase I similarly will not inhibit the capacity of the drugs to intercalate into DNA.

Sequence Selectivity. A DNase I footprinting study was carried out using three DNA restriction fragments of 117, 174, and 265 base pairs labeled at the 3′ end with ^{32}P. With each fragment, the products of digestion by DNase I in the absence and presence of the test drugs were resolved by polyacrylamide gel electrophoresis. Typical gels obtained with AT2433-A1, AT2433-B1, and iso-AT2433-B1 are shown in Fig. 7. The two other uncharged compounds, JDC-108 and

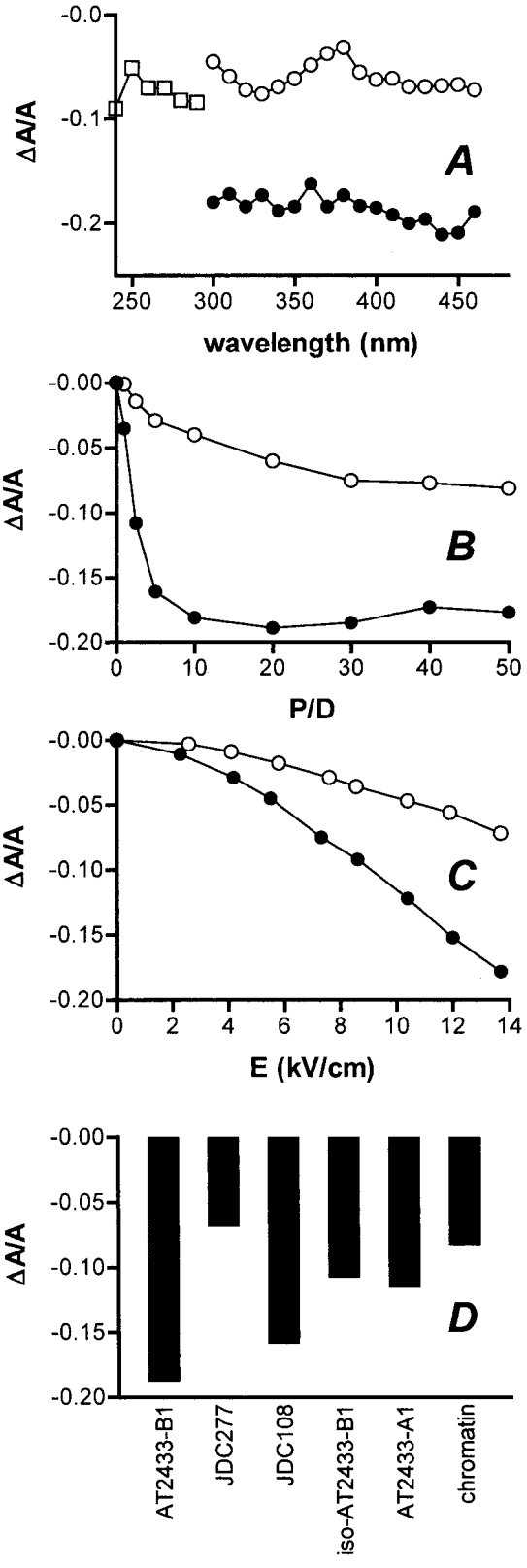

Fig. 6. ELD data for the binding to chromatin. Dependence of the reduced dichroism ΔA/A on the wavelength (A), P/D ratio (B), and electric field strength (C) for AT2433-B1 (●), JDC-277 (○), or DNA alone (□). D, ΔA/A values measured for each drug-chromatin complex at 320 nm or for chromatin alone at 260 nm. Conditions: 13.6 kV/cm, P/D = 25 (250 μM chromatin, 10 μM drug) (A); 320 nm, 13.6 kV/cm (B); 320 nm, P/D = 25 for the DNA-drug complexes and 260 nm for the DNA alone (C) in 1 mM sodium cacodylate buffer, pH 7.0.

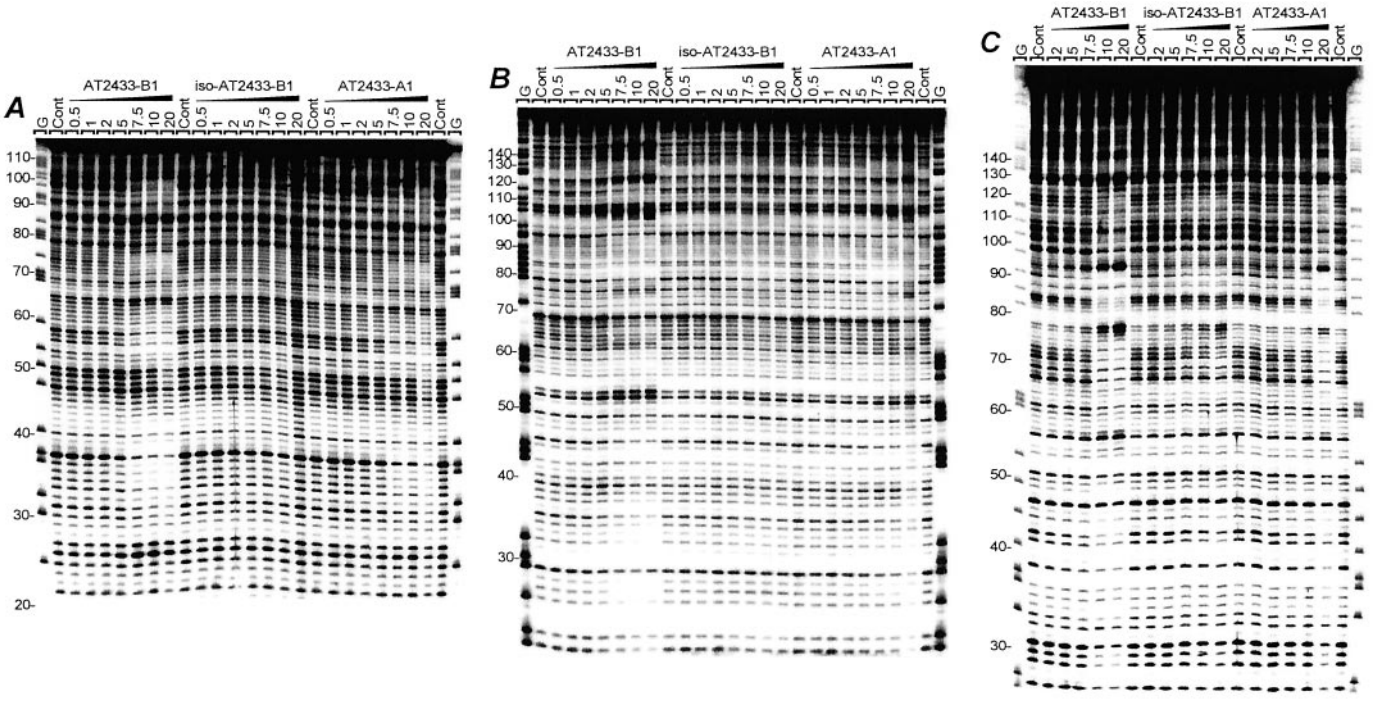

Fig. 7. Sequence selective binding. The three gels show DNase I footprinting with the 117-mer (A), 174-mer (B), and 265-mer *Pvu*II-*Eco*RI restriction fragments (C) in the presence of graded concentrations of AT2433-A1, AT2433-B1, and iso-AT2433-B1. In each case, the DNA was 3′ end-labeled at the *Eco*RI site with α-[^{32}P]dATP in the presence of avian myeloblastosis virus reverse transcriptase. The products of nuclease digestion were resolved on an 8% polyacrylamide gel containing 7 M urea. Control tracks (Cont) contained no drug. Guanine-specific sequence markers obtained by treatment of the DNA with dimethyl sulfate followed by piperidine were run in the lanes marked G. Numbers on the left side of the gel refer to the standard numbering scheme for the nucleotide sequence of the DNA fragment, as indicated in Fig. 8.

JDC-277, showed no effect on the cleavage of DNA by DNase I (data not shown) in sharp contrast to the antibiotic AT2433-B1, which profoundly perturbed the enzyme activity. Both the modification of the orientation of the sugar, as in iso-AT2433-B1, and the addition of a chlorine atom on the indolocarbazole chromophore, as in AT2433-A1, reduce significantly the capacity of the antibiotic to recognize defined sequences in DNA. Band intensities in the different gels were

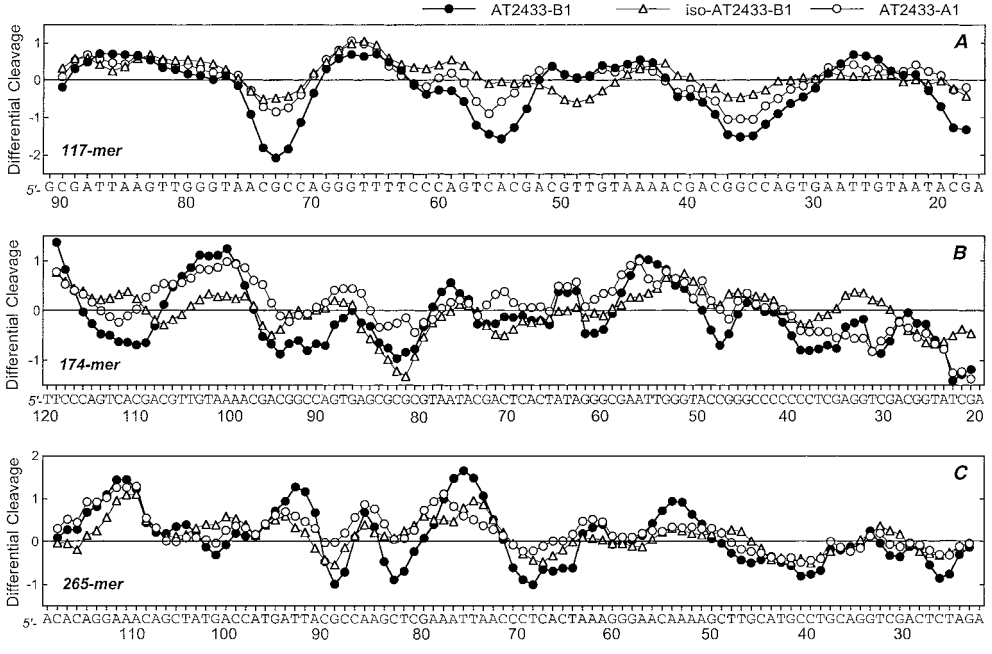

Fig. 8. Differential cleavage plots comparing the susceptibility of the 117-mer (A), 174-mer (B), and 265-mer *Pvu*II-*Eco*RI restriction fragments (C) to DNase I cutting in the presence of AT2433-A1, AT2433-B1, and iso-AT2433-B1 (10 μM each). Deviation of points toward the lettered sequence (negative values) corresponds to a ligand-protected site and deviation away (positive values) represents enhanced cleavage. Vertical scales are in units of $\ln(f_a) - \ln(f_c)$, where f_a is the fractional cleavage at any bond in the presence of the drug and f_c is the fractional cleavage of the same bond in the control, given a closely similar extent of digestion in each case.

quantified by PhosphorImaging to obtain the differential cleavage plots presented in Fig. 8. The comparison between AT2433-B1 and its diastereoisomer fully confirms our previous observations that the configuration of the xylose subunit of the antibiotic is essential to the DNA interaction (Carrasco et al., 2002). The 3*S*,4*S* stereochemistry of the 2,4-dideoxy-4-methylamino-L-xylose subunit of AT2433-B1 seems to be well adapted to the DNA groove surface allowing the antibiotic to bind preferentially to sequences with a high GC content, such as 5′-CGGCCAG, 5′-GTCACG, and 5′-ACGGCC. On the contrary, the 3*R*,4*R* stereochemistry of the sugar moiety of iso-AT2433-B1 is apparently unfavorable for DNA sequence recognition. It is not rare to observe that a modification of the sugar moiety of a DNA binding antibiotic has a profound impact on its capacity to read the genetic information.

Topoisomerase I Inhibition. The effect of the drugs on the catalytic activity of human topoisomerase I was investigated using a conventional plasmid DNA relaxation assay (Bailly, 2001). Two types of effects can be detected depending on the experimental conditions. In the absence of ethidium bromide in the agarose gel during the electrophoresis, the relaxation of supercoiled DNA by topoisomerase I gives a population of topoisomers and the presence of an intercalating agent affects the distribution of the topoisomers population due to an unwinding effect. The typical gel presented in Fig. 9A shows that JDC-277 produces dose-dependent alterations in plasmid linking number. With 5 μM JDC-277, the plasmid becomes fully relaxed and at higher concentrations the accumulation of positive supercoils reflects the unwinding of the DNA typical of an intercalating agent. The unwinding effect was more pronounced with AT2433-B1 than with JDC-277 (data not shown). To better differentiate the specific (poisoning) and nonspecific effects the same experiments were performed in parallel using ethidium bromide-containing agarose gels. In this case, the relaxed DNA migrates faster than the supercoiled plasmid due to ethidium-induced DNA unwinding effects. As shown in Fig. 9B, an increase in the intensity of the band corresponding to nicked DNA molecules can be detected with JDC-277, although the effect is weak compared with what can be achieved with the reference topoisomerase I poison camptothecin (lane CPT in Fig. 9B). However, there is no doubt that JDC-277 stabilizes topoisomerase I-DNA complexes. Similar experiments performed with the five compounds and the results are presented in Fig. 9C. The antibiotic AT2433-B1, which has the highest affinity for DNA in the series, strongly reduces the electrophoretic mobility of the supercoiled DNA band but does not stabilize topoisomerase I-DNA complexes. In contrast, the two compounds with the lowest affinity for DNA, JDC-277 and JDC-108, both induce an increase of the intensity of the band corresponding to the nicked form of DNA. Tight binding to DNA is not required, and even detrimental, for trapping the covalent DNA-topoisomerase I complexes.

DNA restriction fragments were then used to investigate the effect of the compounds on the sequence-specific cleavage of DNA by topoisomerase I. The ^{32}P-radiolabeled DNA fragments were incubated with the test drug and the enzyme and the resulting cleavage products were resolved on sequencing gels so as to identify the sequence of the drug-induced topoisomerase I cleavage sites. Two gels are shown in Fig. 10. In gel A, the five drugs were tested at two concentrations and topoisomerase I-mediated cleavage sites are detected only with JDC-277 and JDC-108 but not with the amino-bisglycoside derivatives. Interestingly, JDC-277 induces topoisomerase I-mediated cleavage essentially at T^{-1} sites, as observed with camptothecin ($T^{\downarrow}G_{137}$, $T^{\downarrow}G_{104}$, $T^{\downarrow}A_{74}$, and $T^{\downarrow}G_{52}$) and is less efficient than NB-506 for inducing cleavage at C^{-1} sites. A comparison with NB-506, which is the lead compound in the indolocarbazole series of topoisomerase I inhibitors

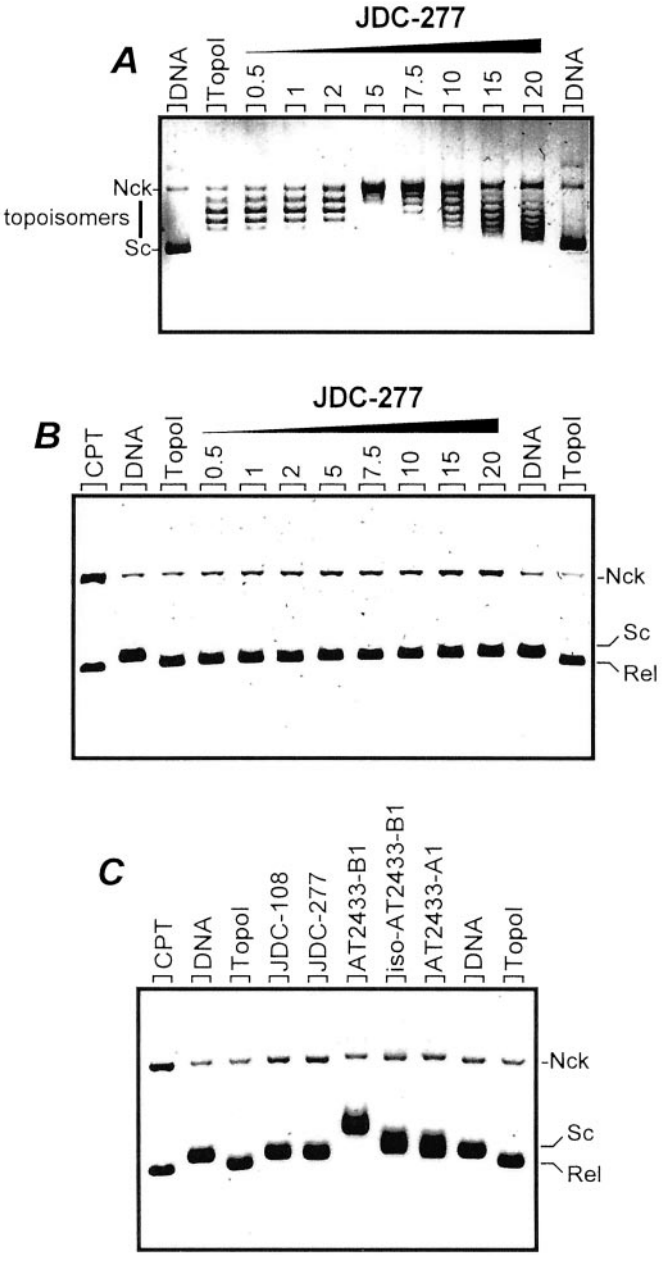

Fig. 9. Topoisomerase I inhibition. Effect of increasing concentrations of JDC-277 on the relaxation of plasmid DNA by human topoisomerase I in the absence (A) or in the presence (B) of ethidium bromide during the electrophoresis. C, effect of the different drugs (20 μM each). Native supercoiled pKMp27 DNA (0.5 μg) (lane DNA) was incubated with 4 units topoisomerase I in the absence (lane TopoI) or presence of drug at the indicated concentration (micromolar). Reactions were stopped with sodium dodecylsulfate and treatment with proteinase K. DNA samples were separated by electrophoresis on 1% agarose gels. The gel was stained with ethidium bromide after the electrophoresis (A) or contained ethidium (1 μg/ml) before the electrophoresis (B and C). Nck, nicked; Rel, relaxed; Sc, supercoiled.

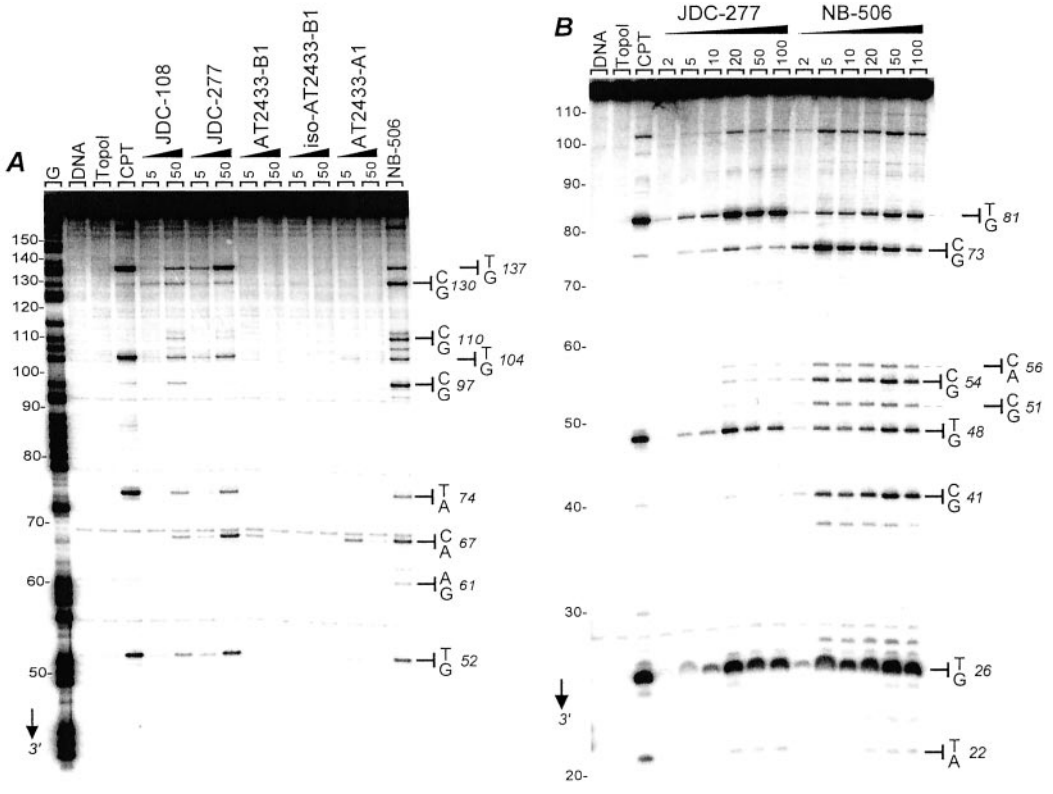

Fig. 10. Cleavage of the 174-mer (A) and the 117-mer DNA fragments (B) by human topoisomerase I in the presence of the indolocarbazoles. In both cases, the 3′ end-labeled fragment (DNA) was incubated in the absence (lane TopoI) or presence of the test drug at the indicated μM concentration. CPT was used at 50 μM. Topoisomerase I cleavage reactions were analyzed on an 8% denaturing polyacrylamide gel. Numbers at the left side of the gels show the nucleotide positions, determined with reference to the guanine tracks labeled G. The nucleotide positions and sequences to the cleavage sites are indicated.

(Bailly et al., 1999a), is shown in Fig. 10B. The profile of DNA cleavage observed with JDC-277 is closer to that of camptothecin than to NB-506. For example, the strong cleavage sites at C$^{\downarrow}$G steps (C$^{\downarrow}$G$_{73}$, C$^{\downarrow}$A$_{56}$, C$^{\downarrow}$G$_{51}$, and C$^{\downarrow}$G$_{41}$) with NB-506 are much weaker with JDC-277. This bis-glycosyl compound behaves as a camptothecin-type inhibitor (weak DNA binding, T^{-1} cleavage preference).

Cytotoxicity. A tetrazolium-based assay was applied to determine the drug concentration required to inhibit cell growth by 50% after incubation in the culture medium for 72 h. The calculated IC_{50} values with the CEM human leukemia cell line are collated in Table 2. The two diglycoside antibiotics AT2433-A1 and AT2433-B1 proved to be the most cytotoxic compounds of the series with IC_{50} values 5 to 10 times lower than that of the uncharged mono and diglycosides JDC-108 and JDC-277. Iso-AT2433-B1 was the least cytotoxic compound with an IC_{50} value 20 times higher than that of the parent diastereoisomer AT2433-B1. The altered configuration of iso-AT2433-B1 is highly detrimental to the cytotoxic action and the substitution of the indolocarbazole chromophore with a chlorine atom also slightly reduces the cytotoxicity.

TABLE 2
Cytotoxicity
Drug concentration that inhibits cell growth by 50% after incubation in liquid medium for 72 hours. Each drug concentration was tested in triplicate, SE of each point is <10%. RRI is the ratio between the CEM/C2-IC_{50} value and the CEM-IC_{50} value.

	IC_{50}		RRI
	CEM	CEM/C2	
	μM		
AT2433-A1	0.29	1.28	4.4
AT2433-B1	0.13	0.41	3.2
iso-AT2433-B1	2.56	5.11	2
JDC-277	1.25	37.55	30
JDC-108	1.83	3.5	1.9
CPT	0.003	7.025	2340
Etoposide	0.28	0.91	3.3

The cytotoxicity assays were repeated with the cell line CEM/C2 selected for its resistance to CPT (Fujimori et al., 1995). The *top1* gene in these cells carries a point mutation adjacent to the catalytic center (Asn722Ser), which makes them poorly sensitive to topoisomerase poisons (Pommier et al., 1999). With this cell line, the cytotoxicity of the AT2433 compounds is only slightly reduced, by a factor of 2 to 4, compared with the parental CEM cell line (Table 2). The same relative resistance index (RRI) was measured with the drug etoposide which is a potent topoisomerase II inhibitor, but has no effect on topoisomerase I. In sharp contrast, the high cytotoxicity of CPT is considerably reduced (RRI >2000) with the *top1*-mutated cell line. The very low IC_{50} value (nanomolar) measured with CPT on the CEM cells can be explained by the fact that this drug is particularly toxic toward human leukemia cells and, unlike the indolocarbazoles, it is a “clean” compound, very

specific for topoisomerase I, with no known additional target.

The two uncharged compounds JDC-108 and JDC-277 that showed an anti-topoisomerase I activity against the purified enzyme in vitro behave differently against the CEM/C2 cell line. The *top1* mutation in those cells has little effect on the cytotoxicity of JDC-108, with a RRI of about 3, as obtained with the AT2433-type compounds. On the contrary, the point mutation of the *top1* gene significantly reduces the cytotoxic potential of the diglycoside JDC-277 with a RRI of 30, i.e., much less than that measured with CPT but 10 times higher than that obtained with etoposide. Together, the cytotoxicity measurements therefore suggest that topoisomerase I is a potential cell target for JDC-277, but not for the other indolocarbazoles tested in this study. However, these data must be considered with caution because the likely existence of additional targets in those CEM cells (e.g., kinases) may underestimate the role of topoisomerase I in the cytotoxic action of these compounds. For example, the reference indolocarbazole NB-506 only gave an RRI of 6 with the same couple of CEM(/C2) cell lines (Urasaki et al., 2001) despite its well established action at the topoisomerase I level in cells (Kanzawa et al., 1995; Komatani et al., 1999).

Cell Cycle Effects. Treatment of human leukemia CEM cells with increasing concentrations of AT2433-B1, but not with its diastereoisomer, for 24 h led to marked changes of the cell cycle profiles (Fig. 11). The flow cytometric analysis of propidium iodide-labeled cells indicates that the treatment with 0.5 μM AT2433-A1 or -B1 induces a significant accumulation of cells in the S phase. The S-cell population increases from 23% in the control to 41% in the presence of 1 μM AT2433-B1. To get a more precise view of the drug effect at the S-phase level, cells were labeled with BrdU, a thymidine analog that incorporates into newly synthesized strands of DNA. As shown in Fig. 12, fewer $BrdU^+$ cells, labeled in S phase at the time of treatment, were detected after 24 h of treatment with AT2433-B1 than in the control cell population. The drug potently inhibits the incorporation of BrdU into DNA and therefore reduces the entry of cells into the vulnerable DNA synthesis phase of the cell cycle. Cells with DNA content less than G1 can be also detected with this compound, and to a lower extent with the chlorinated analog AT2433-A1 (Fig. 11). Sub-G1 cells are usually considered as apoptotic cells (Kluza et al., 2000). No such effects were observed with JDC-277 and with the diastereoisomer iso-AT2433-B1. The cell cycle profiles also remained unchanged, even when using a high drug concentration (data not shown).

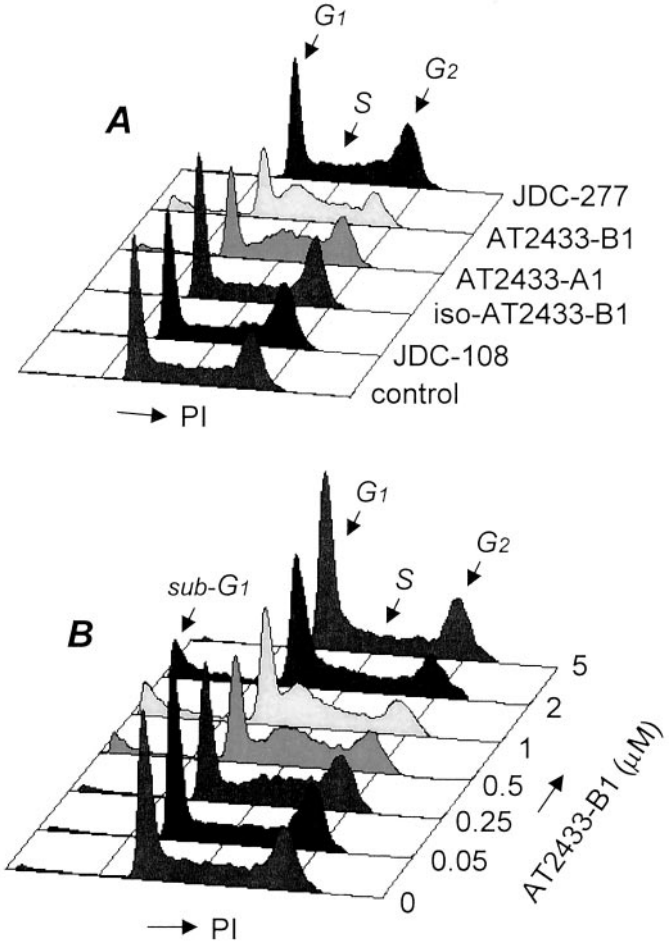

Fig. 11. Cell cycle analysis of CEM human leukemia cells treated for 24 h with the different compounds at 0.5 μM (A) and increasing concentrations of AT2433-B1 (B). Cells were analyzed with the FACScan flow cytometer.

Discussion

The study reported herein was initiated on the basis of the structural analogy between the indolocarbazole diglycoside AT2433-A1 and the indolocarbazole monoglycoside rebeccamycin. We hypothesized that the replacement of the methoxyglucose moiety of rebeccamycin with a 2,4-dideoxy-4-methylamino-L-xylose disaccharide could preserve the capacity of the drug to interact with DNA and topoisomerase I. Not surprisingly, the cationic aminosugar subunit of the AT2433 antibiotics is a positive element for DNA recognition but, unexpectedly, it is unfavorable for topoisomerase I poisoning. In the following section, these two aspects are discussed in turn because we know from our previous studies with different series of indolocarbazole glycosides that DNA interaction and topoisomerase I inhibition are two different

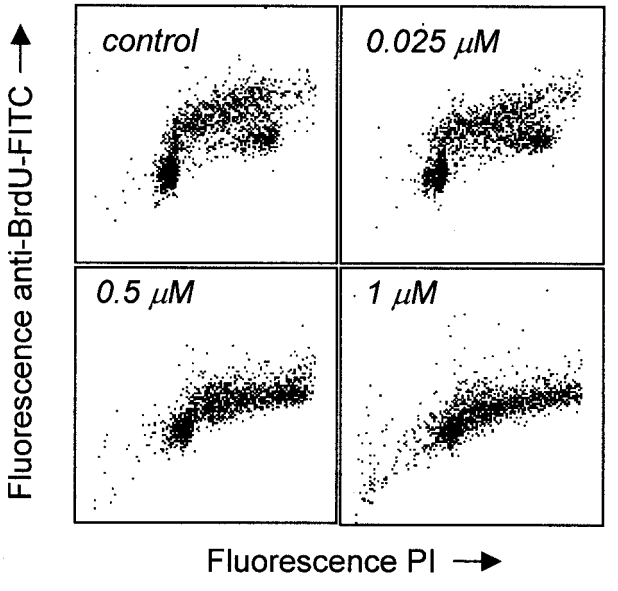

Fig. 12. Modification of bromodeoxyuridine incorporation in CEM cells treated with AT2433-B1. Cells were treated for 24 h with the test drug at the indicated concentrations before labeling with the BrdU-fluorescein isothiocyanate conjugate for 1 h and counterstained with PI.

and essentially unrelated aspects of the molecular mechanism of action of these compounds (Anizon et al., 1997; Bailly et al., 1997, 1999a,b, 2000). In the NB-506 series, it is clear that the drug needs not to intercalate into DNA to inhibit topoisomerase I and exert its cytotoxic activity (Bailly et al., 1999a).

DNA Binding and Sequence Recognition. The mechanism of action of the antibiotic AT2433-A1 had never been studied before the present work. For the last 20 years, this indolocarbazole diglycoside was in some way an orphan drug with no identified molecular target(s). We show herein that DNA is a receptor for AT2433-A1 and its dechlorinated analog AT2433-B1. In a very recent study, we disclosed that AT2433-B1 preferentially recognizes GC-rich sequences in DNA to form very stable, slow-dissociating complexes, whereas its diastereoisomer iso-AT2433-B1 exhibits a very weak sequence preference (Carrasco et al., 2002). The present study extends these observations to confirm that the configuration of the amino-xylose subunit of AT2433-B1 is essential to the DNA interaction. The presence of a chlorine atom on the indolocarbazole ring system slightly reduces the capacity of the drug to interact with DNA. The *T*m and SPR data concur to show that AT2433-B1 binds more tightly to DNA than its chlorinated analog AT2433-A1, which, however, maintains the capacity to discriminate between AT- and GC-rich sequences. These observations are reminiscent to those previously made with rebeccamycin: the removal of the two chlorine atoms significantly promoted DNA intercalation (Bailly et al., 1997). There is no doubt that the cationic diglycoside moiety of the AT2433 antibiotics plays a major role in their tight interaction with DNA. Both the charge and the configuration are important. Altering the orientation of the sugar residue, as in iso-AT2433-B1, and the substitution of a melibiose disaccharide (as in JDC-277) for the aminosugar subunit of AT2433-B1, decreases DNA affinity by a factor of 10 or more, depending on the target sequence.

Stimulation of Topoisomerase I-Mediated DNA Strand Breaks. The replacement of the monoglycoside of rebeccamycin-type compounds with a cationic diglycoside residue is attractive for at least two essential reasons: 1) it potentially offers expanded DNA sequence recognition capacities, and 2) it increases considerably the aqueous solubility of the compounds and therefore should facilitate drug formulation and administration. But these two key points are valid only if the main target of the drug, topoisomerase I, is preserved (unless another drugable target could be identified). This is not the case here. Neither AT2433-A1 nor AT2433-B1 was capable of stimulating topoisomerase I-mediated DNA cleavage. The monoglucoside derivative JDC-108 is a weak inhibitor of topoisomerase I. The addition of a second uncharged sugar residue does not reinforce the interaction with DNA but has a positive impact on the capacity of the drug to inhibit topoisomerase I. Indeed, JDC-277 and JDC-108 exhibit comparable affinities for DNA (as judged from the *T*m data) but the galactose-glucosyl (i.e., melibiose) diglycoside unit of JDC-277 potentiates the DNA nicking activity of topoisomerase I slightly more than the glucosyl monoglycoside JDC-108 (compare the extent of DNA cleavage in Fig. 10A). In sharp contrast, the incorporation of the methyl-amino-xylose carbohydrate unit abolishes topoisomerase I inhibition in spite of the reinforced DNA interaction. The mode of DNA binding rather than the binding affinity may be a critical determinant of topoisomerase I inhibition by indolocarbazole glycosides.

It is interesting to observe that JDC-277 maintains an activity against topoisomerase I. This makes it the first indolocarbazole diglycoside targeting the enzyme. A previous attempt, with a maltosyl (bis-glucose) derivative of NB-506 had resulted in a complete loss of activity against topoisomerase I (Qu et al., 2000). There is therefore hope that one can modulate drug efficacy on the basis on topoisomerase I targeting by virtue of modifying the sugar unit of rebeccamycin. The orientation of the 4″-OH substituent on the second sugar residue may be critical. We can postulate that in the equatorial position (as for glucose) the OH group may not be correctly positioned for stabilizing the topoisomerase I-DNA complex formed transiently whereas in the axial position (as for galactose), the OH might be favorably placed to block the DNA religation of the cleaved strand by the enzyme. This hypothesis is strengthened by previous findings that changes in the stereochemistry of the carbohydrate markedly influence the topoisomerase I inhibitory capacity of indolocarbazole monoglycosides (Bailly et al., 1999c) as well as certain anthracyclines such as nogalamycin and aclacinomycin (Nitiss et al., 1997; Sim et al., 1997; Guano et al., 1999). But so far, the number of glycoside indolocarbazoles known to target the topoisomerase I-DNA complex is relatively limited and no precise structural information is available to offer a rational for the design of carbohydrates recognizing the enzyme and/or the DNA in the ternary complex.

Relation to Cytotoxicity. There is no direct relationship between cytotoxicity and ability to stimulate DNA cleavage by topoisomerase I. The only diglycoside that stimulates DNA cleavage by topoisomerase I, JDC-277, is 10 times less cytotoxic than the parent antibiotic AT2433-B1 devoid of activity against the nuclear DNA relaxing enzyme. Parenthetically, it is worth mentioning that none of the drugs used in this study stabilize topoisomerase II-DNA complexes (data not shown). In contrast, there may be a relationship between cytotoxicity and affinity constants for DNA. The two AT2433 antibiotics that display the highest affinity for GC-rich sequences in DNA are the most cytotoxic compounds. The modification of the stereochemistry of the aminosugar residue provides iso-AT2433-B1, which exhibits a decreased DNA affinity and is also substantially less potent at inhibiting cell growth than the parent antibiotic. To paraphrase the common dogma in the anthracycline series (Arcamone et al., 1997), we can conclude that DNA complexation is certainly an essential step in the sequence of events leading to the inhibition of tumor cells by the indolocarbazole diglycoside antibiotic AT2433. The consideration that DNA interaction contributes to the cytotoxic action of the indolocarbazole diglycosides sets a direction for further work to enhance our understanding of the mechanism of action of these compounds and the development of a new generation of indolocarbazoles that are more effective against tumor cells.

Acknowledgments

We thank C. Bal, B. Baldeyrou, and N. Wattez for outstanding technical assistance. We thank the Institut de Médecine Predictive et de Recherche Thérapeutique (IMPRT) for access to the BiaCore 3000 instrumentation and Prof. D. W. Wilson (Department of Chem-

istry, Georgia State University, Atlanta, GA) for expert assistance with the SPR experiments.

References

Anizon F, Belin L, Moreau P, Sancelme M, Voldoire A, Prudhomme M, Ollier M, Sevère D, Riou JF, Bailly C, et al. (1997) Syntheses and biological activity (topoisomerases inhibition, antitumoral and antimicrobial properties) of rebeccamycin analogues bearing modified sugar moieties and substituted on the imide nitrogen with a methyl group. *J Med Chem* **40:**3456–3465.

Arakawa H, Iguchi T, Morita M, Yoshinari T, Kojiri K, Suda H, Okura A, and Nishimura S (1995) Novel indolocarbazole compound 6-*N*-formylamino-12,13-dihydro-1, 11-dihydroxy-13-(β-D-glucopyranosyl)-5*H*-indolo[2,3-*a*]pyrrolo-[3,4-*c*]carbazole-5,7-(6*H*)-dione (NB-506): its potent antitumor activities in mice. *Cancer Res* **55:**1316–1320.

Arcamone F, Animati F, Capranico G, Lombardi P, Pratesi G, Manzini S, Supino R, and Zunino F (1997) New developments in antitumor anthracyclines. *Pharmacol Ther* **76:**117–124.

Bailly C, Goossens JF, Laine W, Anizon F, Prudhomme M, Ren J, and Chaires JB (2000) Formaldehyde cross-linking of a 2′-aminoglucose rebeccamycin derivative to both A·T and G·C base pairs in DNA. *J Med Chem* **43:**4711–4720.

Bailly C, Dassonneville L, Colson P, Houssier C, Fukasawa K, Nishimura S, and Yoshinari T (1999a) Intercalation into DNA is not required for inhibition of topoisomerase I by indolocarbazole antitumor agents. *Cancer Res* **59:**2853–2860.

Bailly C, Helbecque N, Hénichart JP, Colson P, Houssier C, Rao KE, Shea RG, and Lown JW (1990) Molecular recognition between oligopeptides and nucleic acids. DNA sequence specificity and binding properties of an acridine-linked netropsin hybrid ligand. *J Mol Recognit* **3:**26–35.

Bailly C, Qu X, Chaires JB, Colson P, Houssier C, Ohkubo M, Nishimura S, and Yoshinari T (1999b) Substitution at the F-ring N-imide of the indolocarbazole antitumor drug NB-506 increases the cytotoxicity, DNA binding and topoisomerase I inhibition activities. *J Med Chem* **42:**2927–2935.

Bailly C, Qu X, Graves DE, Prudhomme M, and Chaires JB (1999c) Calories from carbohydrates. Energetic contribution of the carbohydrate moiety of rebeccamycin to DNA binding and the effect of its orientation on topoisomerase I inhibition. *Chem Biol* **6:**277–286.

Bailly C (2001) DNA relaxation and cleavage assays to study topoisomerase I inhibitors. *Methods Enzymol* **340:**610–623.

Bailly C, Riou JF, Colson P, Houssier C, Rodrigues-Pereira E, and Prudhomme M (1997) DNA cleavage by topoisomerase I in the presence of indolocarbazole derivatives of rebeccamycin. *Biochemistry* **36:**3917–3929.

Bailly C and Waring MJ (1995) Comparison of different footprinting methodologies for detecting binding sites for a small ligand on DNA. *J Biomol Struct Dyn* **12:**869–898.

Bush JA, Long BH, Catino JJ, Bradner WT, and Tomita K (1987) Production and biological activity of rebeccamycin, a novel antitumor agent. *J Antibiot (Tokyo)* **40:**668–678.

Carrasco C, Facompré M, Chisholm JD, Van Vranken DL, Wilson WD, and Bailly C (2002) DNA sequence recognition by the indolocarbazole antitumor antibiotic AT2433–B1 and its diastereoisomer. *Nucleic Acids Res* **30:**1774–0781.

Chisholm JD, Golik J, Krishnan B, Matson JA, and Van Vranken DL (1999) A caveat in the application of the exciton chirality method to *N*,*N*-dialkyl amides. Synthesis and structural revision of AT2433–B1. *J Am Chem Soc* **121:**3801–3802.

Chisholm JD and Van Vranken DL (2000) Regiocontrolled synthesis of the antitumor antibiotic AT2433–A1. *J Org Chem* **65:**7541–7553.

Colson P, Bailly C, and Houssier C (1996) Electric linear dichroism as a new tool to study sequence preference in drug binding to DNA. *Biophys Chem* **58:**125–140.

Davis TM and Wilson WD (2000) Determination of the refractive index increments of small molecules for correction of surface plasmon resonance data. *Anal Biochem* **284:**348–353.

Fujimori A, Harker WG, Kohlhagen G, Hoki Y, and Pommier Y (1995) Mutation at the catalytic site of topoisomerase I in CEM/C2, a human leukemia cell line resistant to camptothecin. *Cancer Res* **55:**1339–1346.

Golik J, Doyle TW, Krishnan B, Dubay G, and Matson JA (1989) AT2433–A1, AT2433–A2, AT2433–B1 and AT2433–B2 novel antitumor compounds produced by *Actinomadura melliaura*. II. Structure determination. *J Antibiot (Tokyo)* **42:**1784–1789.

Guano F, Pourquier P, Tinelli S, Binaschi M, Bigioni M, Animati F, Manzini S, Zunino F, Kohlhagen G, Pommier Y, et al. (1999) Topoisomerase poisoning activity of novel disaccharide anthracyclines. *Mol Pharmacol* **67:**77–84.

Hagmar P, Marquet R, Colson P, Kubista M, Nielsen P, Norden B, and Houssier C (1989) Electric and flow linear dichroism of unfolded and condensed chromatin: a comparative study at low and intermediate ionic strength. *J Biomol Struct Dyn* **7:**19–33.

Houssier C (1981) Investigating nucleic acids, nucleoproteins, polynucleotides and their interactions with small ligands by electro-optical systems, in *Molecular Electro-Optics* (Krause S ed.) pp. 363–398, Plenum Press, New York.

Kanzawa F, Nishio K, Kubota N, and Saijo N (1995) Antitumor activities of a new indolocarbazole substance, NB-506 and establishment of NB-506-resistant cell lines, SBC-3/NB. *Cancer Res* **55:**2806–2813.

Kluza J, Lansiaux A, Wattez N, Mahieu C, Osheroff N, and Bailly C (2000) Apoptotic response of HL-60 human leukemia cells to the antitumor drug TAS-103. *Cancer Res* **60:**4077–4084.

Komatani H, Morita M, Sakaizumi N, Fukasawa K, Yoshida E, Okura A, Yoshinari T, and Nishimura S (1999) A new mechanism of acquisition of drug resistance by partial duplication of topoisomerase I. *Cancer Res* **59:**2701–2708.

Matson JA, Claridge C, Bush JA, Titus J, Bradner WT, Doyle TW, Horan AC, and Patel M (1989) AT2433–A1, AT2433–A2, AT2433–B1 and AT2433–B2, novel antitumor antibiotic compounds produced by *Actinomadura malliaura*. *J Antibiot (Tokyo)* **42:**1547–1555.

Nettleton DE, Doyle TW, Krishnan B, Matsumoto GK, and Clardy J (1985) Isolation and structure of rebeccamycin: a new antitumor antibiotic from *Nocardia aerocolonigenes*. *Tetrahedron Lett* **26:**4011–4014.

Nitiss JL, Pourquier P, and Pommier Y (1997) Aclacinomycin A stabilizes topoisomerase I covalent complexes. *Cancer Res* **57:**4564–4569.

Pommier Y, Pourquier P, Urasaki Y, Wu J, and Laco GS (1999) Topoisomerase I inhibitors: selectivity and cellular resistance. *Drug Resist Updat* **2:**307–318.

Qu X, Chaires JB, Ohkubo M, Yoshinari T, Nishimura S, and Bailly C (2000) A DNA-binding indolocarbazole disaccharide derivative remains highly cytotoxic without inhibiting topoisomerase I. *Anticancer Drug Des* **14:**433–442.

Sim SP, Gatto B, Yu C, Liu AA, Li TK, Pilch DS, LaVoie EJ, and Liu LF (1997) Differential poisoning of topoisomerases by menogaril and nogalamycin dictated by the minor groove-binding nogalose sugar. *Biochemistry* **36:**13285–13291.

Urasaki Y, Laco G, Takebayashi Y, Bailly C, Kohlhagen G, and Pommier Y (2001) Use of camptothecin-resistant mammalian cell lines to evaluate the role of topoisomerase I in the antiproliferative activity of the indolocarbazole, NB-506 and its topoisomerase I binding site. *Cancer Res* **61:**504–508.

Woo MH, Vance JR, Otero Marcos AR, Bailly C, and Bjornsti M-A (2002) Active site mutations in DNA topoisomerase I distinguish the cytotoxic activities of camptothecin of camptothecin and the indolocarbazole, rebeccamycin. *J Biol Chem* **277:**3813–3822.

Yoshinari T, Matsumoto M, Arakawa H, Okada H, Noguchi K, Suda H, Okura A, and Nishimura S (1995) Novel antitumor indolocarbazole compound 6-*N*-formylamino-12,13-dihydro-1,11-dihydroxy-13-(β-D-glucopyranosyl)-5*H*-indolo[2,3-*a*]pyrrolo-[3,4-*c*]carbazole-5,7-(6*H*)-dione (NB-506): induction of topoisomerase I-mediated DNA cleavage and mechanisms of cell line-selective cytotoxicity. *Cancer Res* **55:**1310–1315.

Address correspondence to: Christian Bailly, INSERM U-524, Laboratoire de Pharmacologie Antitumorale, du Centre Oscar Lambret, IRCL, 59045 Cedex Lille, France. E-mail: bailly@lille.inserm.fr